International Journal of Applied Mathematics
Volume 1 No. 4 1999, 411 - 438

FORCED VIBRATION OF A SDOF SYSTEM WITH A NEW HYSTERETIC DAMPING SUBJECTED TO HARMONIC LOADING

S. R. Kuo and J. T. Chen *
Dept. of Harbor and River Engineering, Taiwan Ocean University
Keelung, TAIWAN
e-mail: B0209@ntou66.ntou.edu.tw
* Address for correspondence: P.O. Box 7-59
Keelung, TAIWAN

Abstract: The periodic solution for the new hysteretic damping model subjected to harmonic loading is analytically derived. The numerical solution using the Runge-Kutta method from the transient state to steady state is worked out for verification. The hysteresis loop is constructed and the dissipation energy of the area is shown to be indepedent of the exciting frequency theoretically and numerically. The stability and convergence for the perturbation of the initial disturbance are demonstrated by means of a numerical example using the Runge-Kutta method. The phase lags between input and output for different ranges of loss factors and exciting frequencies are examined. Also, the sticking phenomenon when the external force can not overcome the friction damping is discussed. The subharmonic solution is worked out using the numerical method.

AMS Subj. Classification: 73F99, 73K12, 70J05, 70J35; 65L06
Key Words: hysteretic damping, dissipation, forced vibration, sticking and subharmonic solution

1. Introduction

The damping characteristic is often utilized to suppress the vibration level using various energy dissipation mechanisms. Damping models, *e.g.*, viscous, Coulomb and hysteresis damping, have been discussed in detail in the literature of structural dynamics and viscoelasticity. A great deal of effort has been

Received: May 4, 1999

focused on the frequency domain approach, especially for the hysteretic damping model. Free vibration of a single degree of freedom(SDOF) system with hysteretic damping was solved by Chen *et al.* [1]. Although the model in [1] obeys the casual effect, Crandall [2] criticized this model for not being fully equivalent to the hysteretic damping model in the frequency domain. A "new" hysteretic damping model was suggested for the model in [1] by Crandall. In 1980's, there was renewed interest in the model with the addition of Coulomb damping so that it modelled the behavior of elastometric bearings used in base isolation [3]. The equivalent linearization for the nonlinear hysteretic system was also studied in [4]. By taking the Fourier transform with respect to the nonlinear model in [1], one can not obtain the complex stiffness of $k(1 + i\eta)$. The above statement confirms that Crandall's comment in [2] is right. Also, this finding stimulated research on the time-domain formulation for the linear hysteretic damping reported in [5, 6], where the inverse Fourier transform for the model was considered in the frequency domain. It is interesting that Chen's study [5, 6] and Inaudi's work [7] both independently derived the same integro-differential equation(IDE) for the linear hysteretic model in the time domain. For the new nonlinear model mentioned in Crandal's paper, Caughy and his coworkers [8] also solved its free and forced vibration. Later, Makris and Constantinou have solved the the steady state solution of multiple-stops for linear/Coulomb friction model [3]. However, they did not focus on the dissipation mechanism and subharmonic response.

In this paper, we extend the free vibration to forced vibration for harmonic loading of the new hysteretic damping in the time domain for all ranges of exciting frequencies. The hysteresis loop is constructed in the phase plane to understand the disspation behavior. The transient behavior from initial state to steady state on the damping ellipse is found by using the Runge-Kutta method. Also, the steady state solution is analytically derived without considering the initial conditions. The stability and convergence for the perturbation of initial disturbance on the steady-state solution are numerically verified. To demonstrate that the present model is also hysteretic, the relation between the dissipation energy and exciting frequency is considered. The sticking phenomenon is also discussed, and the phase lag between the input and output for different loss factors and exciting frequencies is examined. Also, the subharmonic response is demonstrated by means of a numerical experiment using the Runge-Kutta method.

2. Formulation of the Forced Vibration Subjected to Harmonic Loading

The definition of hysteretic damping has been given by Clough and Penzien [9], where the damping force is proportional to the amplitude of the displacement,

u, and is in phase with the velocity, $\dot{u}$. Therefore, the damping force, f_d, of a SDOF system can be expressed as

$$f_d \equiv h\frac{|u|}{|\dot{u}|}\dot{u}, \tag{1}$$

where h is a proportional constant. The governing equation for the forced vibration of a SDOF system can be derived as

$$m\ddot{u} + h\frac{|u|}{|\dot{u}|}\dot{u} + ku = P(t). \tag{2}$$

When $P(t)$ is the external force and is set to be $\bar{P}e^{i\alpha t}$, the steady state solution, $u = \bar{u}e^{i\alpha t}$, is expected. Although Eq.(2) is nonlinear, it has been wrongly reformulated in the frequency domain as follows [10]:

$$-m\alpha^2\bar{u} + k(1 \pm i\eta)\bar{u} = \bar{P}, \quad + \ when \ \alpha > 0, - \ when \ \alpha < 0, \tag{3}$$

where $\bar{u}$ and $\bar{P}$ are the Fourier transforms for u and P, respectively, and $k(1\pm i\eta)$ denotes the complex stiffness with η denoting the loss factor:

$$\eta = \frac{h}{k}. \tag{4}$$

When $\alpha > 0$, the complex stiffness reduces to $k(1 + i\eta)$, which is the conventional complex stiffness. Crandall [2] mentioned that eqs.(2) and (3) are not equivalent mathematically. Now we will focus on the problem in the time domain with the following governing equation:

$$m\ddot{u}(t) + k\eta\frac{|u|}{|\dot{u}|}\dot{u}(t) + ku(t) = P(t). \tag{5}$$

For the linear hysteretic damping model, we have the following governing equation [5, 6],

$$\ddot{u}(t) - \frac{\bar{\eta}\omega_0^2}{\pi}\int_{-\infty}^{\infty}\frac{u(\tau)}{(t-\tau)}d\tau + \omega_0^2 u(t) = \frac{P(t)}{m}, \tag{6}$$

where $\bar{\eta}$ is loss factor for linear hysteretic model and

$$\omega_0 = \sqrt{\frac{k}{m}}. \tag{7}$$

By taking Fourier transform with respect to eq.(6), we can obtain the hysteretic damping model in the frequency model as shown in eq.(3). The dissipation energy per cycle of hysteresis was determined as [6]

$$D = \pi k\bar{\eta}\Delta_0^2, \tag{8}$$

where Δ_0 is the maximum response as shown in Fig.1. For the nonlinear hysteretic damping model in eq.(5), Caughy *et al.* [8] derived

$$D = 2k\eta\Delta_0^2. \tag{9}$$

It is found that both models obey the definition of the hysteretic damping model; that is, the dissipation energy per cycle of hysteresis loop should be independent of the exciting frequency. To make the dissipation in eqs.(8) and (9) equal for comparion, we have

$$\eta = \pi\bar{\eta}/2. \tag{10}$$

3. Formulation for the Periodic Solution of the New Hysteretic Damping Model Subjected to Harmonic Excitation – No Sticking

Assume a periodic solution exists under the harmonic loading $P(t) = P_0 \sin(\alpha t)$; we have

$$\alpha t_3 = \alpha t_1 + \pi, \tag{11}$$

where α is the exciting frequency, and t_1, t_2 and t_3 are the time parameters shown in the phase plane of Fig.1 since

$$P(t) = P(t+T), \tag{12}$$

$$P(t) = -P(t+\frac{T}{2}), \tag{13}$$

where T is the period with $T = 2\pi/\alpha$. By setting the two natural frequencies in the four quadrants [?], we have

$$\omega_1^2 = (1+\eta)\omega_0^2, \text{ for the first and third quadrants,} \tag{14}$$

$$\omega_2^2 = (1-\eta)\omega_0^2, \text{ for the second and fourth quadrants.} \tag{15}$$

In the first quadrant, the general solution for eq.(5) contains two parts, complementary and particular solutions, as shown below:

$$u_1(t) = A_1 \sin\alpha t + a_1 \sin\omega_1(t-t_1) + b_1 \cos\omega_1(t-t_1), \tag{16}$$

where a_1 and b_1 are the coefficients to be determined and A_1 is

$$A_1 = \frac{\frac{P_0}{k}}{-\frac{\alpha^2}{\omega_0^2} + (1+\eta)}. \tag{17}$$

In a way similar to that in the second quadrant, we have

$$u_2(t) = A_2 \sin\alpha t + a_2 \sin\omega_2(t_3-t) + b_2 \cos\omega_2(t_3-t), \tag{18}$$

where a_2 and b_2 are the coefficients to be undetermined and A_2 is

$$A_2 = \frac{\frac{P_0}{k}}{-\frac{\alpha^2}{\omega_0^2} + (1-\eta)}. \tag{19}$$

By introducing a new coefficient V_0 as shown in Fig.1 and the two conditions

$$u_1(t_1) = 0, \tag{20}$$

$$u_2(t_3) = 0, \tag{21}$$

we can obtain

$$u_1(t) = A_1[\sin\alpha t - \sin(\alpha t_1)\cos\omega_1(t-t_1)$$

$$-\frac{\alpha\cos(\alpha t_1)}{\omega_1}\sin\omega_1(t-t_1)] + \frac{V_0}{\omega_1}\sin\omega_1(t-t_1), \tag{22}$$

$$u_2(t) = A_2[\sin\alpha t - \sin(\alpha t_3)\cos\omega_2(t-t_3)$$

$$-\frac{\alpha\cos(\alpha t_3)}{\omega_2}\sin\omega_2(t-t_3)] - \frac{V_0}{\omega_2}\sin\omega_2(t-t_3), \tag{23}$$

where

$$V_0 = \dot{u}_1(t_1) = -\dot{u}_2(t_3). \tag{24}$$

In the case of no sticking on the displacement axis in the phase plane, the velocities, $\dot{u}_1(t)$ and $\dot{u}_2(t)$, are both zero at t_2 as follows:

$$\dot{u}_1(t_2) = A_1[\alpha\cos\alpha t_2 + \omega_1\sin(\alpha t_1)\sin\omega_1(t_2-t_1)$$

$$-\alpha\cos(\alpha t_1)\cos\omega_1(t_2-t_1)] + V_0\cos\omega_1(t_2-t_1) = 0, \tag{25}$$

$$\dot{u}_2(t_2) = A_2[\alpha\cos\alpha t_2 + \omega_2\sin(\alpha t_3)\sin\omega_2(t_2-t_3)$$

$$-\alpha\cos(\alpha t_3)\cos\omega_2(t_2-t_3)] - V_0\cos\omega_2(t_2-t_3) = 0. \tag{26}$$

By introducing a new variable, $\triangle_0$, as shown in Fig.1, we obtain

$$u_1(t_2) \equiv \triangle_0 = A_1[\sin(\alpha t_2) - \sin(\alpha t_1)\cos\omega_1(t_2-t_1)$$

$$-\frac{\alpha\cos(\alpha t_1)}{\omega_1}\sin\omega_1(t_2-t_1)] + \frac{V_0}{\omega_1}\sin\omega_1(t_2-t_1), \tag{27}$$

$$u_2(t_2) \equiv \triangle_0 = A_2[\sin(\alpha t_2) - \sin(\alpha t_3)\cos\omega_2(t_2-t_3)$$

$$-\frac{\alpha\cos(\alpha t_3)}{\omega_2}\sin\omega_2(t_2-t_3)] - \frac{V_0}{\omega_2}\sin\omega_2(t_2-t_3). \tag{28}$$

To cancel out the V_0 terms involved in eqs. (25) and (27), we have

$$\triangle_0 = A_1\{\sin\alpha t_2 - \frac{\alpha\cos\alpha t_2}{\omega_1\cos[\omega_1(t_2-t_1)]}\sin\omega_1(t_2-t_1) - \frac{\sin(\alpha t_1)}{\cos\omega_1(t_2-t_1)}\}. \quad (29)$$

In a similar way, we obtain

$$\triangle_0 = A_2\{\sin\alpha t_2 - \frac{\alpha\cos\alpha t_2}{\omega_2\cos[\omega_2(t_2-t_3)]}\sin\omega_2(t_2-t_3) - \frac{\sin(\alpha t_3)}{\cos\omega_2(t_2-t_3)}\} \quad (30)$$

by cancelling out the V_0 terms involved in eqs.(26) and (28).

After introducing the phase angles, θ_1, θ_2 and θ_3 as

$$\theta_1 \equiv \alpha t_1, \quad (31)$$

$$\theta_2 \equiv \alpha t_2, \quad (32)$$

$$\theta_3 \equiv \alpha t_3 = \pi + \theta_1, \quad (33)$$

the above two equations can be rewritten as

$$\triangle_0 = A_1\{\sin\theta_2 - \frac{\cos\theta_2\sin\lambda_1(\theta_2-\theta_1)}{\lambda_1\cos\lambda_1(\theta_2-\theta_1)} - \frac{\sin(\theta_1)}{\cos\lambda_1(\theta_2-\theta_1)}\}, \quad (34)$$

$$\triangle_0 = A_2\{\sin\theta_2 - \frac{\cos\theta_2\sin\lambda_2(\theta_2-\theta_3)}{\lambda_2\cos\lambda_2(\theta_2-\theta_3)} - \frac{\sin\theta_3}{\cos\lambda_2(\theta_2-\theta_3)}\}, \quad (35)$$

where

$$\lambda_1 = \sqrt{1+\eta}\frac{\omega_0}{\alpha}, \quad (36)$$

$$\lambda_2 = \sqrt{1-\eta}\frac{\omega_0}{\alpha}. \quad (37)$$

Dividing eq.(25) by $\cos\omega_1(t_2-t_1)$, V_0 can be represented as

$$V_0 = A_1[\alpha\cos(\alpha t_1) - \frac{\alpha\cos(\alpha t_2)}{\cos\omega_1(t_2-t_1)} - \frac{\omega_1\sin\alpha t_1}{\cos\omega_1(t_2-t_1)}\sin\omega_1(t_2-t_1)]. \quad (38)$$

Dividing eq.(26) by $\cos\omega_2(t_2-t_3)$, V_0 can be represented as

$$V_0 = A_2[-\alpha\cos(\alpha t_3) + \frac{\alpha\cos\alpha t_2}{\cos\omega_2(t_2-t_3)} + \frac{\omega_2\sin\alpha t_3}{\cos\omega_2(t_2-t_3)}\sin\omega_2(t_2-t_3)]. \quad (39)$$

By substituting eqs.(31) $\sim$ (33) into eq.(38), we have

$$V_0 = \alpha A_1[\cos\theta_1 - \frac{\cos\theta_2}{\cos\lambda_1(\theta_2-\theta_1)} - \frac{\lambda_1\sin\lambda_1(\theta_2-\theta_1)}{\cos\lambda_1(\theta_2-\theta_1)}\sin\theta_1]. \quad (40)$$

In a similar way, we have

$$V_0 = \alpha A_2[-\cos(\theta_3) + \frac{\cos\theta_2}{\cos\lambda_2(\theta_2-\theta_3)} + \frac{\lambda_2 \sin\lambda_2(\theta_2-\theta_3)}{\cos\lambda_2(\theta_2-\theta_3)}\sin\theta_3]. \tag{41}$$

By introducing a new variable, δ, to relate θ_1 and θ_2 as

$$\delta \equiv \theta_2 - \theta_1 - \frac{\pi}{2}, \tag{42}$$

we have the following relations:

$$\cos\lambda_2(\theta_2-\theta_3) = \cos\lambda_2(\frac{\pi}{2}-\delta), \tag{43}$$

$$\sin\lambda_2(\theta_2-\theta_3) = -\sin\lambda_2(\frac{\pi}{2}-\delta), \tag{44}$$

$$\cos\theta_2 = -\sin(\theta_1+\delta), \tag{45}$$

$$\sin\theta_2 = \cos(\theta_1+\delta). \tag{46}$$

It must be noted that the range of δ is limited by

$$-\frac{\pi}{2} < \delta < \frac{\pi}{2}. \tag{47}$$

Substituting eqs.(43) $\sim$ (46) into eqs.(34), (35), (40) and (41), we have

$$\triangle_0 = A_1[\cos(\theta_1+\delta) + \frac{\sin(\theta_1+\delta)\sin\lambda_1(\frac{\pi}{2}+\delta)}{\lambda_1\cos\lambda_1(\frac{\pi}{2}+\delta)} - \frac{\sin\theta_1}{\cos\lambda_1(\frac{\pi}{2}+\delta)}], \tag{48}$$

$$\triangle_0 = A_2[\cos(\theta_1+\delta) - \frac{\sin(\theta_1+\delta)\sin\lambda_2(\frac{\pi}{2}-\delta)}{\lambda_2\cos\lambda_2(\frac{\pi}{2}-\delta)} + \frac{\sin\theta_1}{\cos\lambda_2(\frac{\pi}{2}-\delta)}], \tag{49}$$

$$V_0 = \alpha A_1[\cos\theta_1 + \frac{\sin(\theta_1+\delta)}{\cos\lambda_1(\frac{\pi}{2}+\delta)} - \frac{\lambda_1\sin\theta_1\sin\lambda_1(\frac{\pi}{2}+\delta)}{\cos\lambda_1(\frac{\pi}{2}+\delta)}], \tag{50}$$

$$V_0 = \alpha A_2[\cos\theta_1 - \frac{\sin(\theta_1+\delta)}{\cos\lambda_2(\frac{\pi}{2}-\delta)} + \frac{\lambda_2\sin\theta_1\sin\lambda_2(\frac{\pi}{2}-\delta)}{\cos\lambda_2(\frac{\pi}{2}-\delta)}]. \tag{51}$$

In order to solve eqs.(48) $\sim$ (51) with four unknowns, $\triangle_0, V_0, \theta_1$ and δ, the four equations can be rearranged as

$$\triangle_0 = A_1 g_1(\delta)cos(\theta_1) + A_1 h_1(\delta)sin(\theta_1), \tag{52}$$

$$\triangle_0 = A_2 g_2(\delta)cos(\theta_1) + A_2 h_2(\delta)sin(\theta_1), \tag{53}$$

$$V_0 = A_1 f_1(\delta)cos(\theta_1) + A_1 e_1(\delta)sin(\theta_1), \tag{54}$$

$$V_0 = A_2 f_2(\delta)cos(\theta_1) + A_2 e_2(\delta)sin(\theta_1), \tag{55}$$

where $g_1(\delta), g_2(\delta), h_1(\delta), h_2(\delta), e_1(\delta), e_2(\delta)\ f_1(\delta)$ and $f_2(\delta)$ can be easily determined according to eqs.(48) $\sim$ (51). Cancelling out the θ_1, Δ_0 and V_0 terms, we have

$$2(A_1 - A_2)(\frac{A_1}{\cos\mu_1} + \frac{A_2}{\cos\mu_2}) - (A_1 - A_2)[A_1(\lambda_1 + \frac{1}{\lambda_1})\tan\mu_1$$
$$+A_2(\lambda_2 + \frac{1}{\lambda_2})\tan\mu_2]\cos\delta + \{2(A_1^2 + A_2^2)$$
$$-2A_1A_2[1 - \frac{1}{\cos\mu_1\cos\mu_2} + \frac{1}{2}(\frac{\lambda_2}{\lambda_1} + \frac{\lambda_1}{\lambda_2})\tan\mu_1\tan\mu_2]\}\sin\delta = 0,$$

where μ_1 and μ_2 are the functions of δ defined as follows:

$$\mu_1 \equiv \lambda_1(\frac{\pi}{2} + \delta), \tag{56}$$

$$\mu_2 \equiv \lambda_2(\frac{\pi}{2} - \delta). \tag{57}$$

Eq. (56) can be rearranged to get

$$2(\frac{A_1}{\cos\mu_1} + \frac{A_2}{\cos\mu_2}) - [A_1(\lambda_1 + \frac{1}{\lambda_1})\tan\mu_1 + A_2(\lambda_2 + \frac{1}{\lambda_2})\tan\mu_2]\cos\delta$$
$$+2(A_1 - A_2)\sin\delta + \frac{2A_1A_2}{A_1 - A_2}[1 + \frac{1}{\cos\mu_1\cos\mu_2}$$
$$-\frac{1}{2}(\frac{\lambda_2}{\lambda_1} + \frac{\lambda_1}{\lambda_2})\tan\mu_1\tan\mu_2]\sin\delta = 0.$$

Only one variable δ left in eq.(59) should be solved. The root of δ for the nonlinear equation can be easily found using the numerical method.

4. Formulation for the Periodic Solution of the New Hysteretic Damping Model Subjected to Harmonic Excitation – Sticking

Substituting t_2 obtained in the above section into $P(t)$, we have

$$P(t_2) = P_0\sin(\alpha t_2). \tag{58}$$

When $\dot{u}(t_2) = 0$, at this moment, only two situations may occur as shown in Fig.2: one is that the state bumps backward to the first quadrant with $\ddot{u}(t) > 0$, and the other is that the state penetrates into the fourth quadrant with $\ddot{u}(t) < 0$. The first case implies that

$$P(t_2) \geq (1 + \eta)k\Delta \tag{59}$$

while the second case implies that

$$P(t_2) \leq (1-\eta)k\Delta. \tag{60}$$

It is interesting to consider what will happen if $P(t_2)$ is in the range of two bounds, *i.e.*,

$$(1-\eta)k\Delta \leq P(t) \leq (1+\eta)k\Delta. \tag{61}$$

The answer is that the mass will stick on the displacement axis with zero velocity since the magnitude of the forces combining the spring force, $k\Delta$, and the external force, $P(t)$, can not overcome the damping force to pull backward in bd curve in Fig.2. It is impossible to pull forward into the fourth quadrant since the velocity, $\dot{u}(t)$, is negative. Therefore, it corresponds to a frozen point in the phase plane mathematically and represents the sticking phenomenon physically. Since the mass will rest in the phase plane as shown in Fig.2, we need to introduce a new variable, t_2^* or θ_2^*. From t_2^* to t_2, the mass rests, and we have

$$P(t_2) = (1-\eta)k\Delta_0. \tag{62}$$

Substituting eqs.(60), (19) and (37) into eq.(64), we have

$$\Delta_0 = A_2 \frac{-1+\lambda_2^2}{\lambda_2^2} \sin\theta_2. \tag{63}$$

Substituting eq.(65) into (35) to cancel the Δ_0 term, we have

$$\frac{-1+\lambda_2^2}{\lambda_2^2}\sin\theta_2 = \sin\theta_2 - \frac{\cos\theta_2 \sin\lambda_2(\theta_2-\theta_3)}{\lambda_2\cos\lambda_2(\theta_2-\theta_3)} - \frac{\sin\theta_3}{\cos\lambda_2(\theta_2-\lambda_3)}. \tag{64}$$

Eq.(66) can be simplified to

$$\tan\theta_2 = \frac{\lambda_2[\sin\lambda_2(\theta_2-\theta_3) - \lambda_2\sin(\theta_2-\theta_3)]}{\cos\lambda_2(\theta_2-\theta_3) - \lambda_2^2\cos(\theta_2-\theta_3)}. \tag{65}$$

Substituting eq.(65) into eq.(34), where θ_2 is replaced by θ_2^* in the first quadrant, we have

$$\frac{-1+\lambda_1^2}{\lambda_2^2}\sin\theta_2 = \sin\theta_2^* - \frac{\cos\theta_2^* \sin\lambda_1(\theta_2^*-\theta_1)}{\lambda_1\cos\lambda_1(\theta_2^*-\theta_1)} - \frac{\sin\theta_1}{\cos\lambda_1(\theta_2^*-\theta_1)}. \tag{66}$$

Cancelling the V_0 terms in eqs.(40) and (41) in a similar way, we have

$$\begin{aligned} &-\cos\theta_3 + \frac{\cos\theta_2}{\cos\lambda_2(\theta_2-\theta_3)} + \frac{\lambda_2\sin\lambda_2(\theta_2-\theta_3)}{\cos\lambda_2(\theta_2-\theta_3)}\sin\theta_3 \\ &= \frac{A_1}{A_2}\left[\cos\theta_1 - \frac{\cos\theta_2^*}{\cos\lambda_1(\theta_2^*-\theta_1)} - \frac{\lambda_1\sin\lambda_1(\theta_2^*-\theta_1)}{\cos\lambda_1(\theta_2^*-\theta_1)}\sin\theta_1\right]. \end{aligned} \tag{67}$$

In summary, we have the three unknowns, θ_1, θ_2 and θ_2^*, to be solved in three equations (67) $\sim$ (69). Note that $\theta_3 = \theta_1 + \pi$. Once θ_1, θ_2 and θ_2^* are available, Δ_0 can be calculated by eq.(65) and V_0 can be determined by eq.(41). The steps in the numerical algorithm for solving the simultaneous system of nonlinear equations for the three unknowns are summarized below:

Step 1:
Initial guess for the value of $\theta_2 - \theta_3$.
Step 2:
According to Eq.(67), θ_2 can be determined directly. Of course, θ_3 can be determined by means of the guess value of step 1 and $\theta_1 = \theta_3 - \pi$.
Step 3:
Substituting θ_1, θ_2 and θ_3 into Eq.(68), we can obtain θ_2^* by iteration.
Step 4:
Substituting $\theta_1, \theta_2, \theta_3$ and θ_2^* into Eq.(69), the half method can be employed to iterate the initial guess of $\theta_2 - \theta_3$. Go to Step 1.

5. Numerical Examples and Discussions

In this section, forced vibration problems will be considered.

Case 1: No sticking ($\alpha = 0.8, \eta = 0.05, \omega_0 = 1, P_0 = 1$).

In this case, no sticking occurs. Fig.3(a) shows the steady state trajectory in the phase plane. The displacement and velocity histories are shown in Figs.3(b) and 3(c), respectively. Fig.3(d) shows the trajectory in the phase plane from the initial state at the origin to steady state using the Runge-Kutta method. Fig.3(e) shows the trajectory in the phase plane from the initial state at $(-0.2, 2.2)$ to steady state using the Runge-Kutta method. The stability of the steady state solution and the convergence can be demonstrated based on Figs.3(d) and 3(e).

Case 2: Sticking ($\alpha = 0.1, \eta = 0.05, \omega_0 = 1, P_0 = 1$).

In this case, the sticking phenomenon occurs. Fig.4(a) shows the steady state trajectory in the phase plane. It is found that the intrinsic time at the same position of B and B^* is different in the phase plane. In another words, the mass rests from the time t_2^* to t_2. The displacement and velocity histories are shown in Figs.4(b) and 4(c), respectively. Fig.4(b) shows that the displacement remains constant during the time from t_2^* to t_2 while Fig.4(c) shows the zero velocity during the same duration. Fig.4(d) shows the trajectory in the phase plane from the initial state at the origin to steady state using the Runge-Kutta method. The stability and the convergence can be demonstrated by Fig.4(d).

Discussion on dissipation energy: ($\omega_0 = 1, P_0 = 2.53$)

According to the above relation, we can design two tables. Table 1 shows the maximum response, strain energy, dissipation energy and loss factors for both models with different loss factors under the same harmonic loadings,

$P(t) = sin(\pi t)$. It is interesting to find that the maximum response decreases as the loss factor increases for the linear model. However, the nonlinear model contradicts this trend. The reason will be explained by considering the phase lag between the input and output. In Table 2, the dissipation energy is found to be indepedent of the exciting frequencies, $\alpha = 0.5\pi, \pi, 1.5\pi$ and 2π, for both linear and nonlinear models. It is found that the amplitudes of the force are different so that we have the same maximum response of one. As the excitation frequency increases, the maximum response decreases for the nonlinear model. For the case of the linear model, the maximum response increases as the exciting frequency increases. The reason can be found by considering the phase lag between the input and output as follows.

Discussion of phase lag: $(\alpha = 1.0, \eta = 1.90, \omega_0 = 1, P_0 = 2.53)$

Setting the exciting frequency constant ($\alpha = 0.5$) for the case of $\omega_0 = 1$, the phase lag between the input and output for different values of loss factors ($\eta = 0.1 \sim 1.8$) is that shown in Fig.5(a). The phase lags can be found from the positions of the symbols in Fig.5(a). When $0.1 < \eta < 0.8$ in Fig.5(a), the phase lag increases as η increases. The phase lag explains why the case with a larger loss factor has larger response since the power efficiency is larger. In the range of $1.0 < \eta < 1.8$ in Fig.5(a), the phase lag remains constant. The larger the loss factor is, the lower the maximum response will be. The displacement and velocity histories are shown in Figs.5(b) and 5(c), respectively.

Setting the loss factor constant ($\eta = 1.0$) for the case of $\omega_0 = 1$, the phase lag between input and output for different values of loss factors ($\alpha = 0.2 \sim 1.5$) is that shown in Fig.6(a). The phase lags can be found from the positions of the symbols in Fig.6(a). When $0.2 < \alpha < 0.5$ in Fig.6(a), the phase lag remains constant. As the excitation frequency approaches more closely the natural frequency, ω_0, a larger response is obtained. In the range of $0.8 < \alpha < 1.5$ in Fig.6(a), the phase lag increases as the exciting frequency increases. The phase lag behaves in a way similar to the viscous damping system. The displacement and velocity histories are shown in Figs.6(b) and 6(c), respectively.

Discussion on subharmonic response:

In the formulation, we assume a harmonic solution with frequency α for the forcing function $P_0 sin(\alpha t)$. We can extend the harmonic solution to a subharmonic solution by introducing more equations for more unknowns in the phase plane. Avoiding the lengthy derivation in analytical way, we have demonstrated that the subharmonic solution exists by using numerical method. For the case of $\alpha = 1.0$ and $\eta = 1.9$, the subharmonic motion can be found by using the Runge-Kutta method. Fig.7(a) shows the trajectory for the subharmonic response in the phase plane. The displacement and velocity histories are shown in Figs.7(b) and 7(c), respectively.

6. Concluding Remarks

The present paper has extended the free vibration of hysteretic damping to forced vibration. The closed-form solution for the steady state solution of the hysteretic damping model subjected to harmonic loading has been obtained for all ranges of exciting frequencies. It has been proved analytically and numerically that the dissipation energy is independent of the exciting frequency if the maximum response is the same. The sticking phenomenon, subharmonic response and phase lag between the input and output have all been discussed. In addition, stability has been demonstrated by means of a numerical example using the Runge-Kutta method.

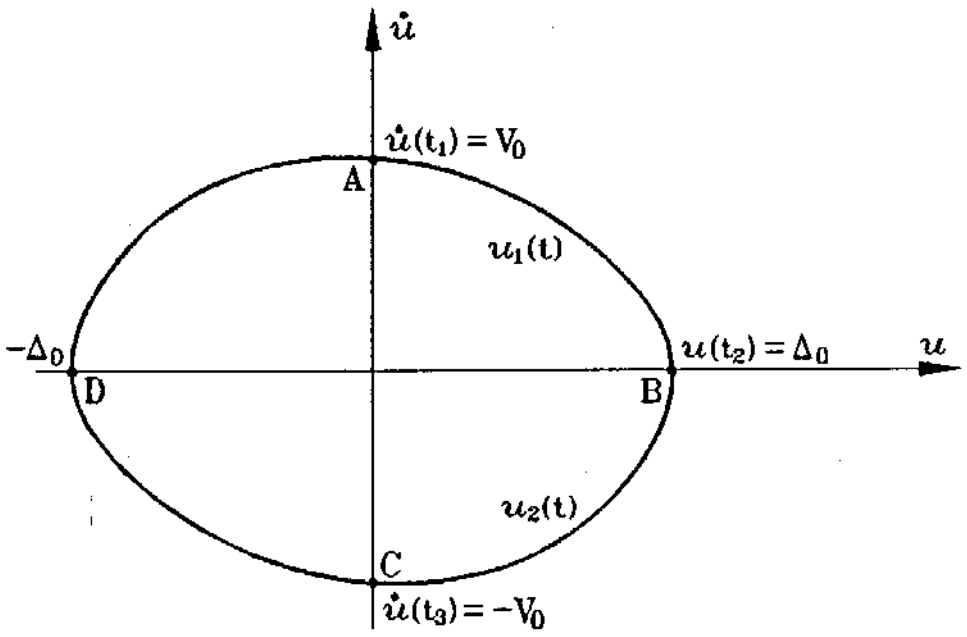

Fig.1: A diagram for typical hysteretic damping under harmonic excitation

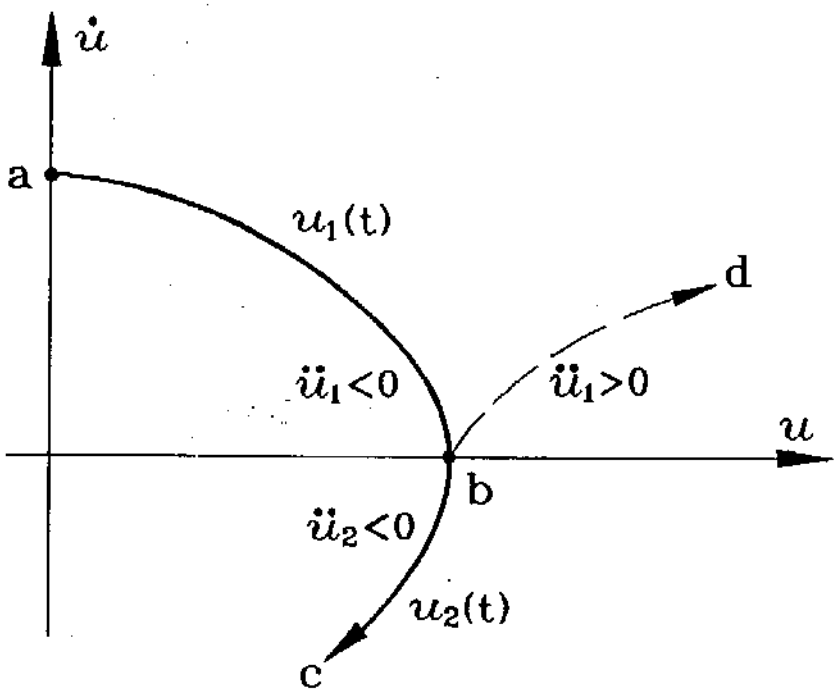

Fig.2: The sticking condition on the displacement axis in the phase plane

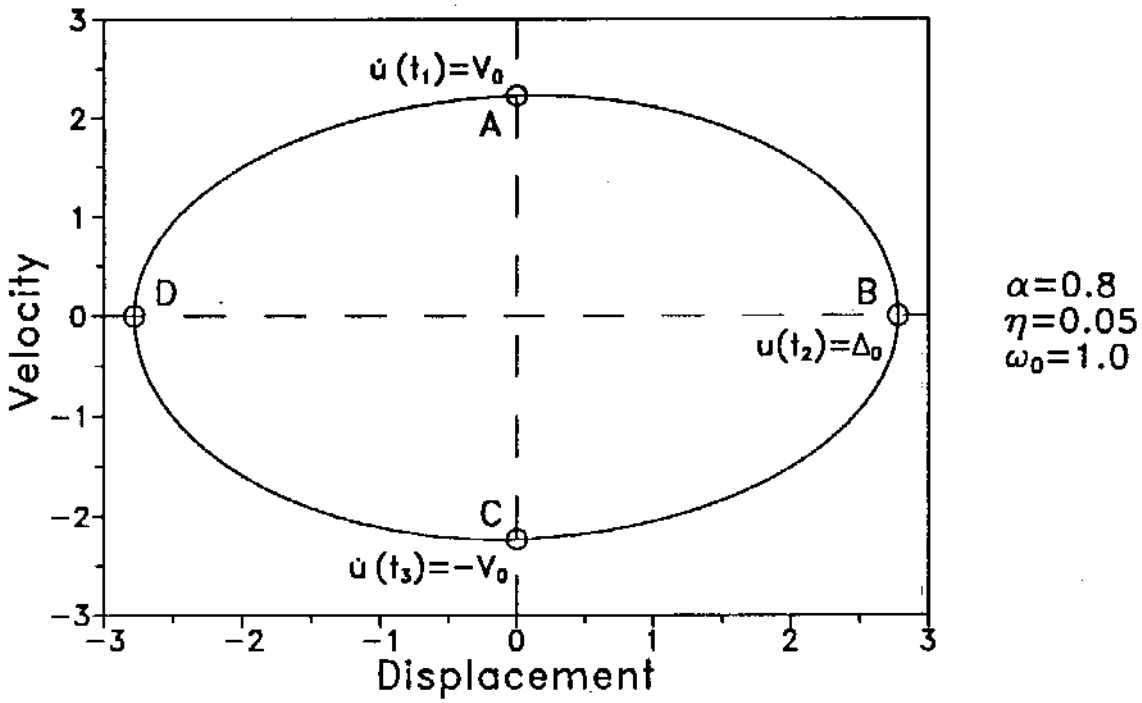

Fig.3: No sticking case ($\alpha = 0.8, \eta = 0.05, \omega_0 = 1$).
(a). steady state trajectory in the phase plane obtained using analytical method

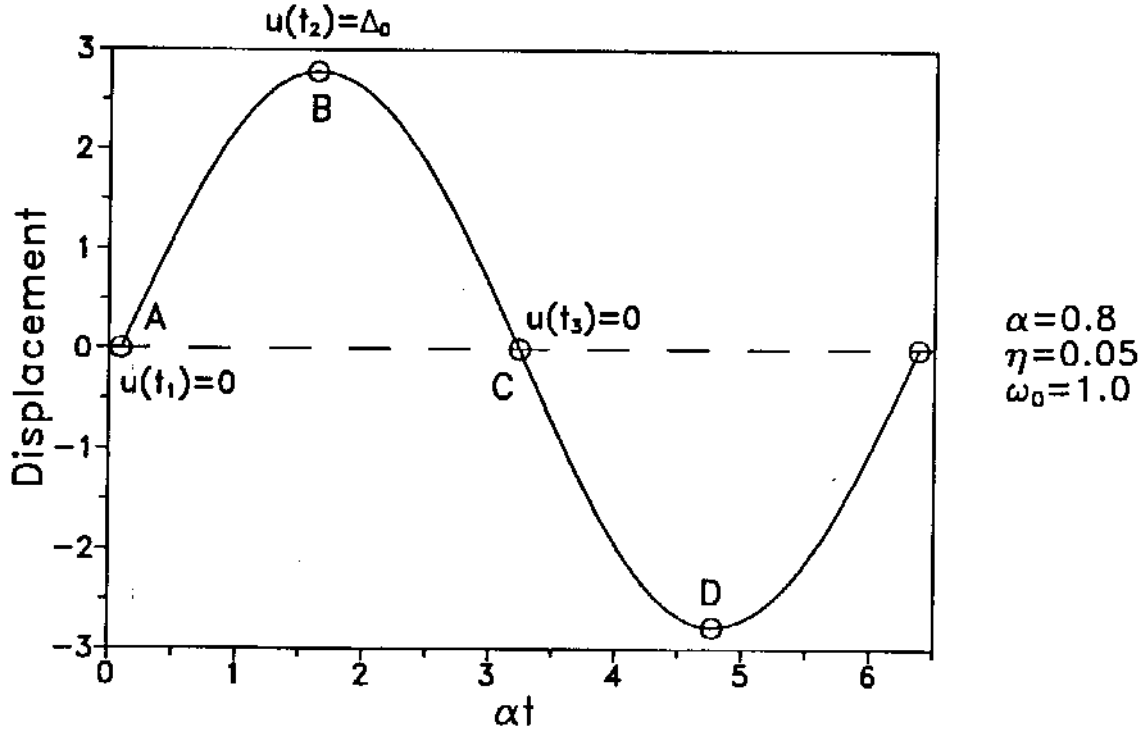

Fig.3: (b). displacement history

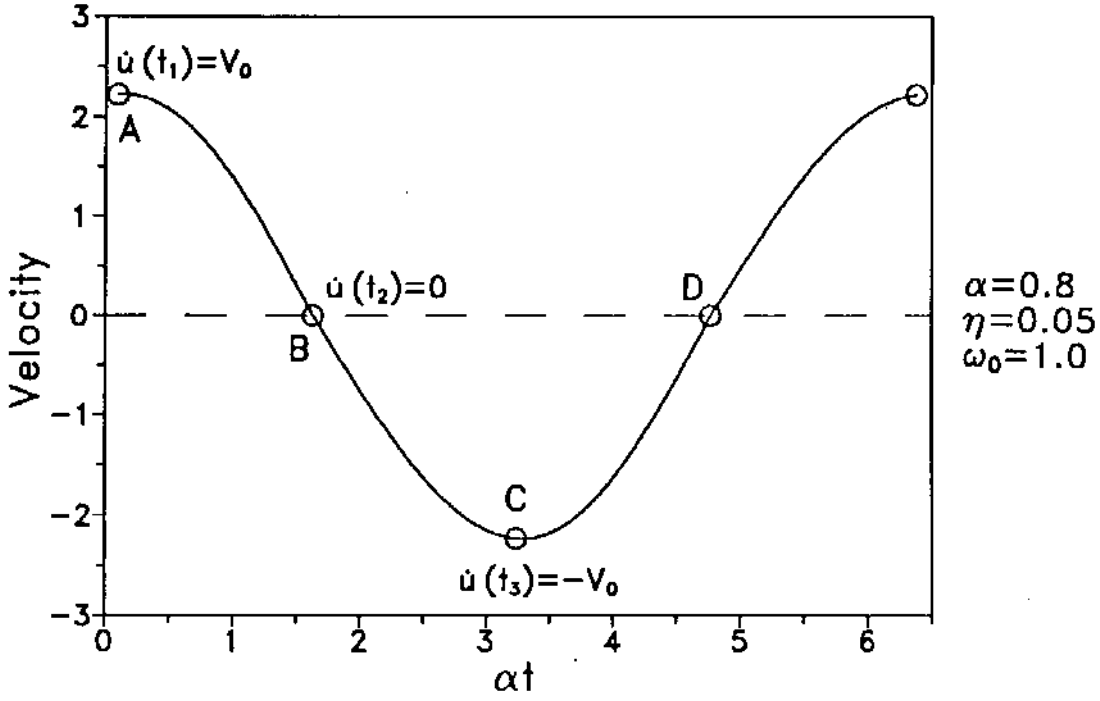

Fig.3: (c). velocity history

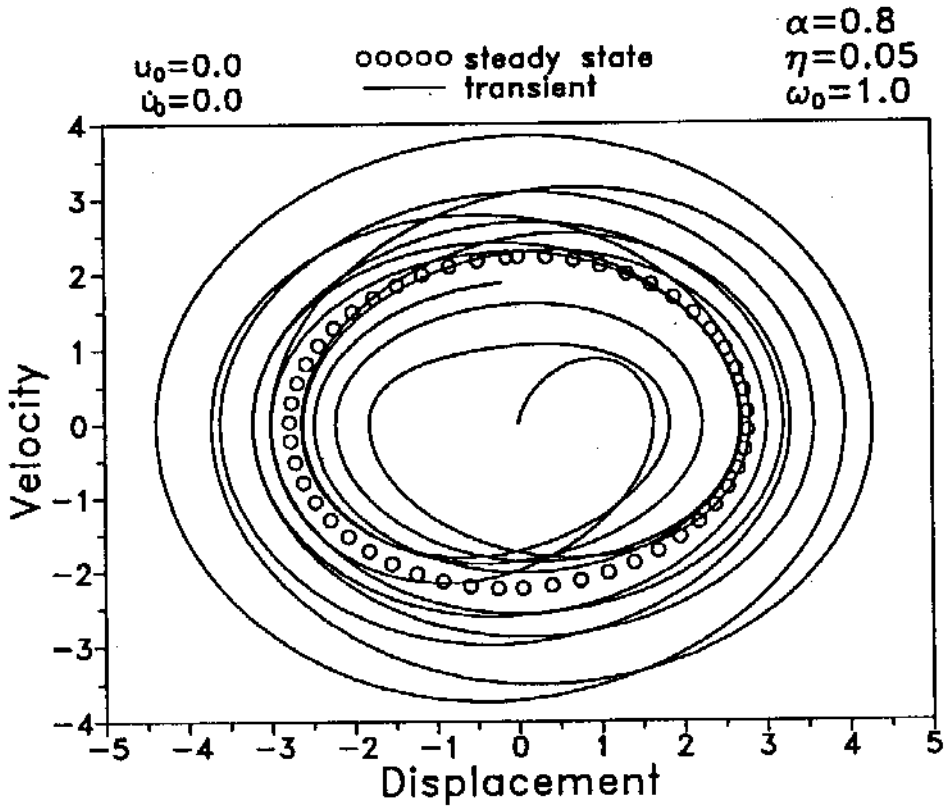

Fig.3: (d). trajectory from the initial state of $(0, 0)$ to steady state using the Runge-Kutta method

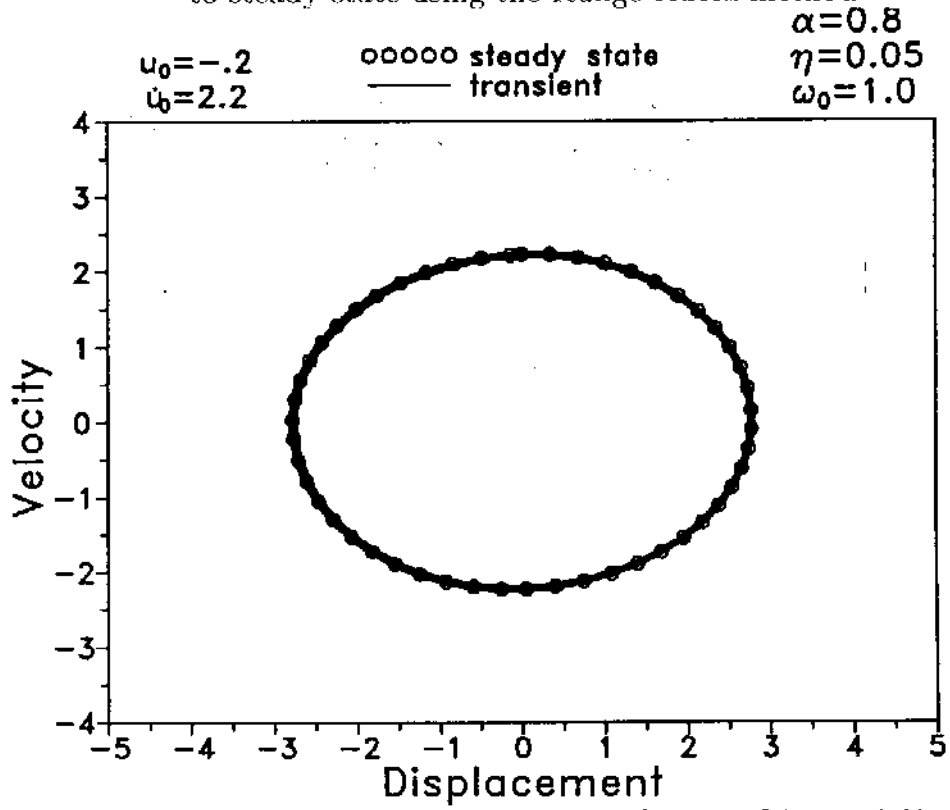

Fig.3: (e). trajectory from the initial state of $(-0.2, 2.2)$ to steady state using the Runge-Kutta method

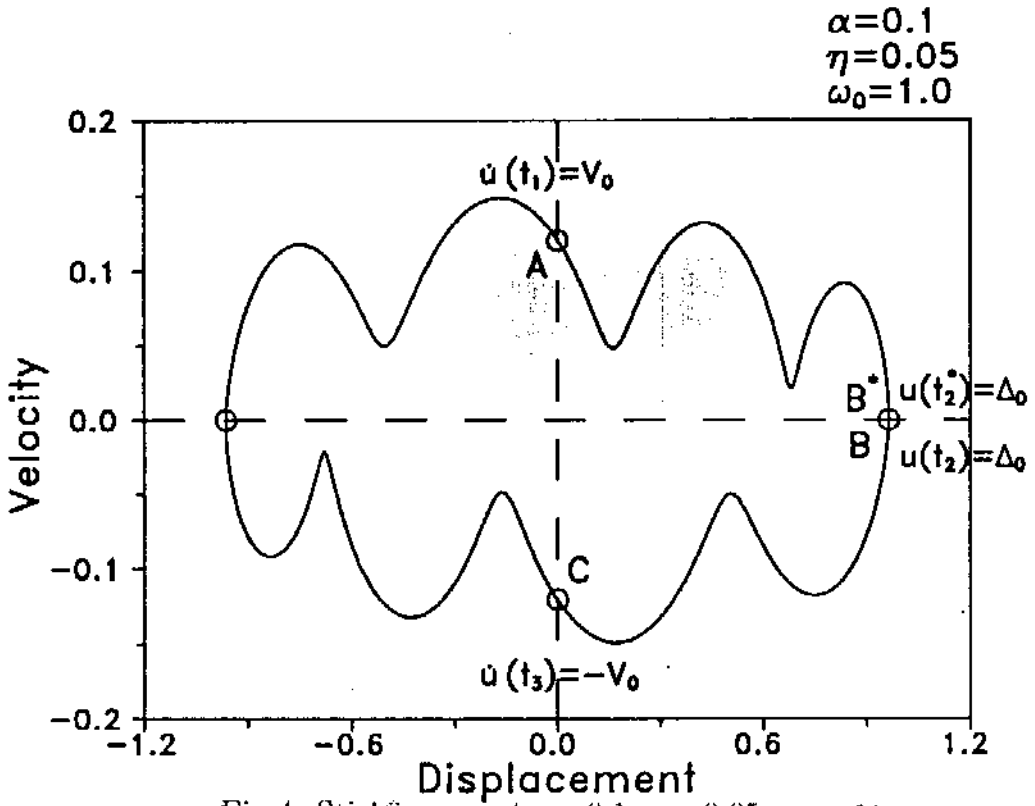

Fig.4: Sticking case ($\alpha = 0.1, \eta = 0.05, \omega_0 = 1$).
(a). steady state trajectory in the phase plane obtained using analytical method

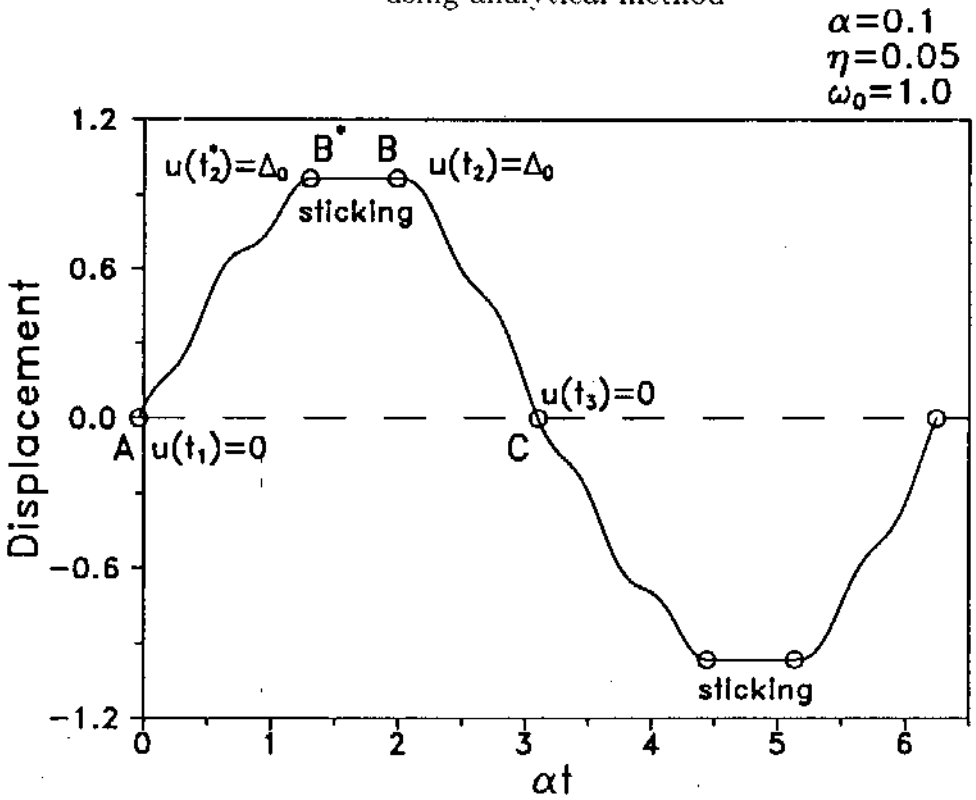

Fig.1: (b). displacement history

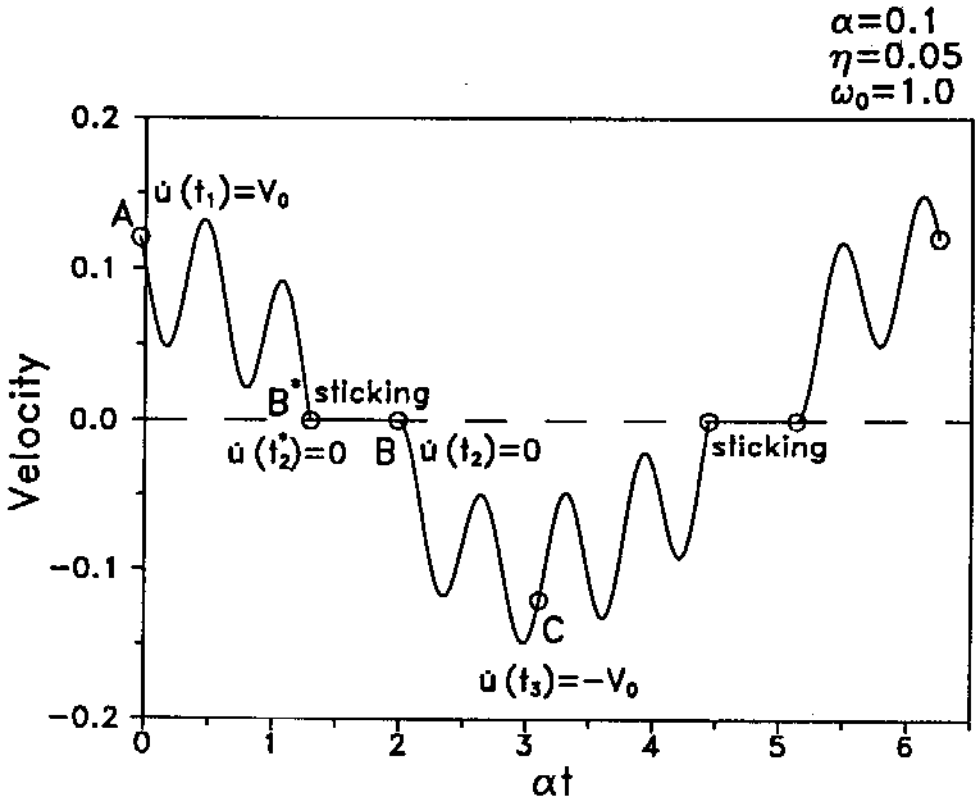

Fig.4: (c). velocity history

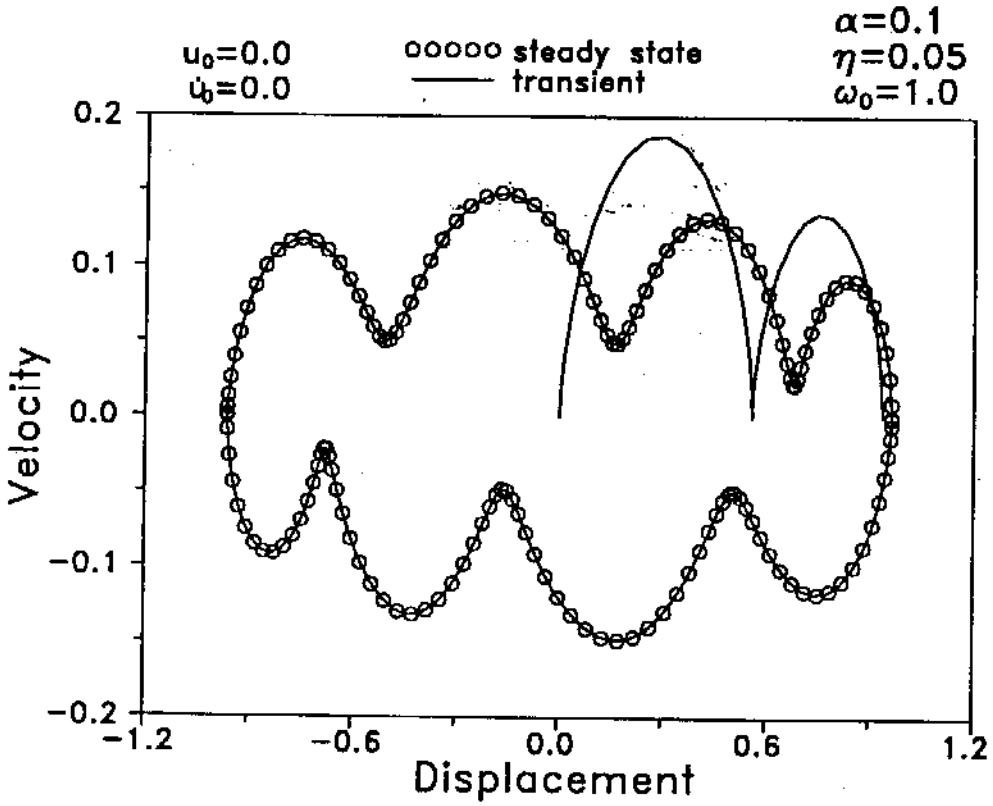

Fig.4: (d). trajectory from the initial state of $(0, 0)$ to steady state using the Runge-Kutta method

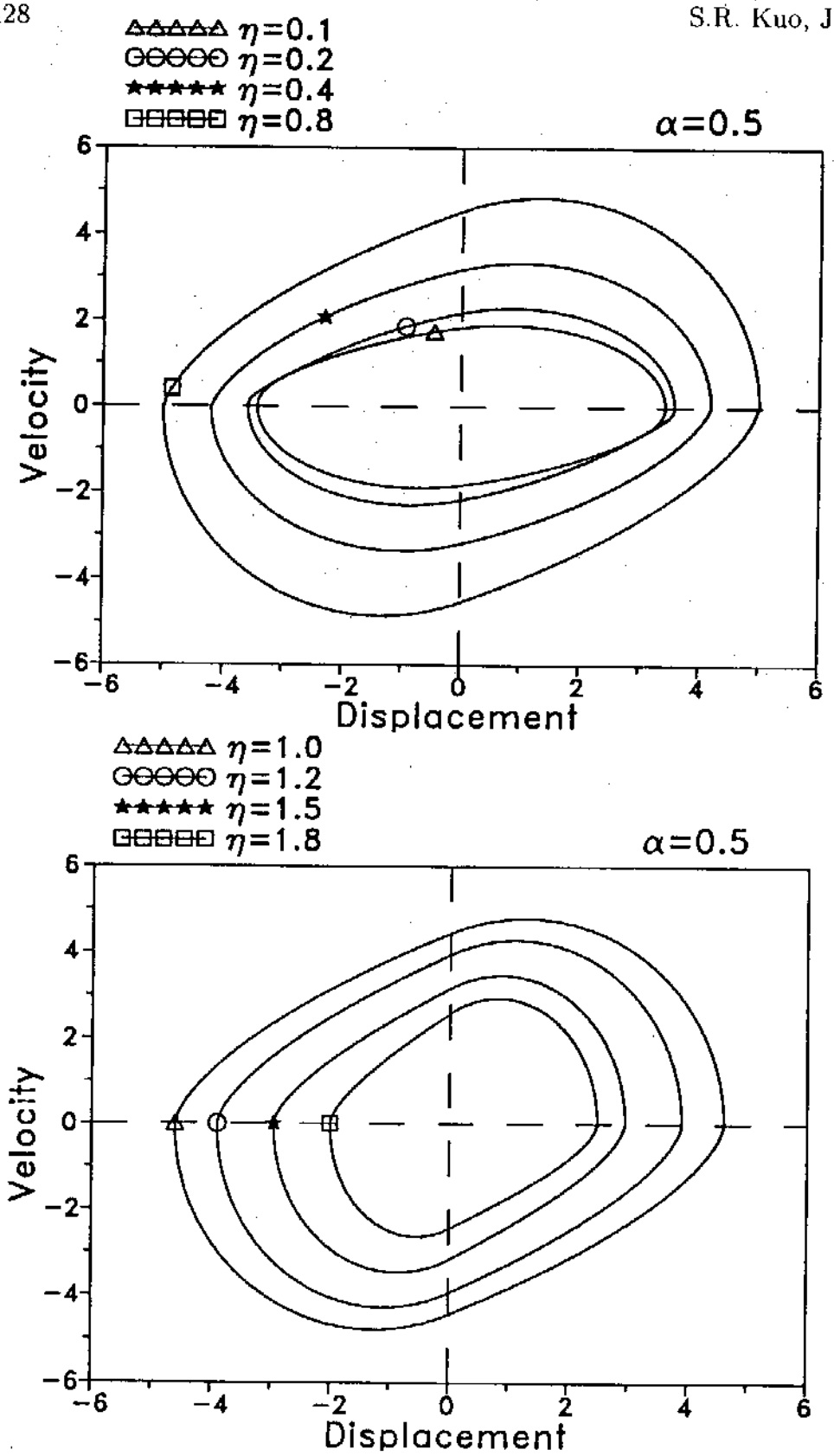

Fig.5: The phase lag between the input and output ($\alpha = 0.5, \omega_0 = 1$).
(a). steady state trajectory in the phase plane

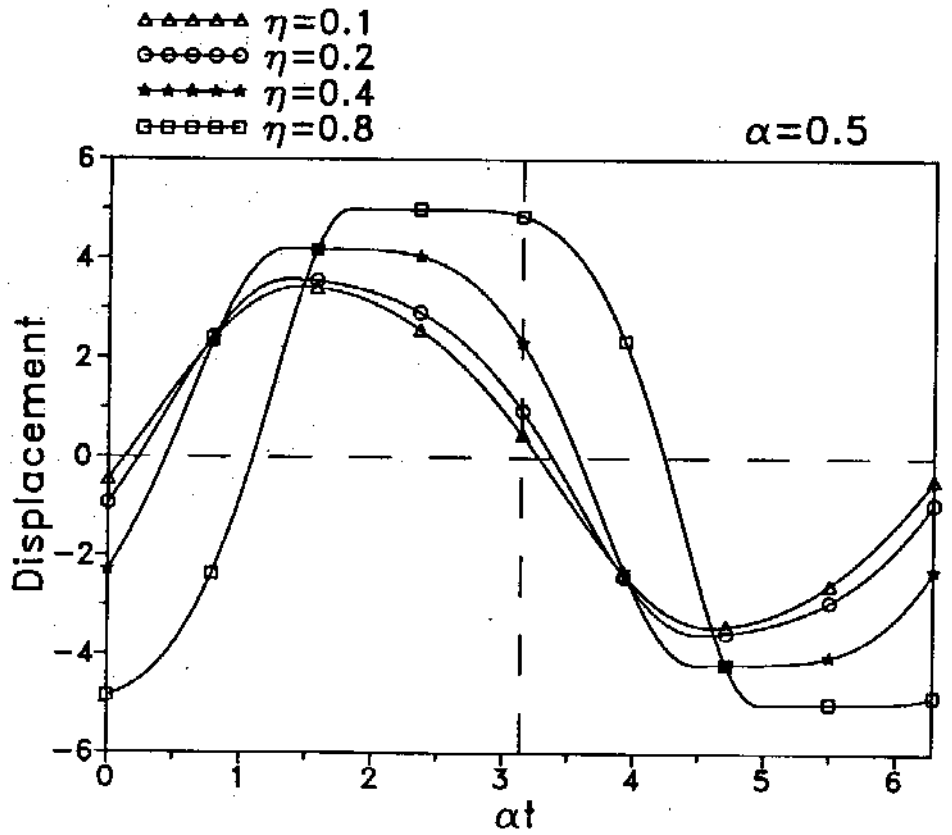

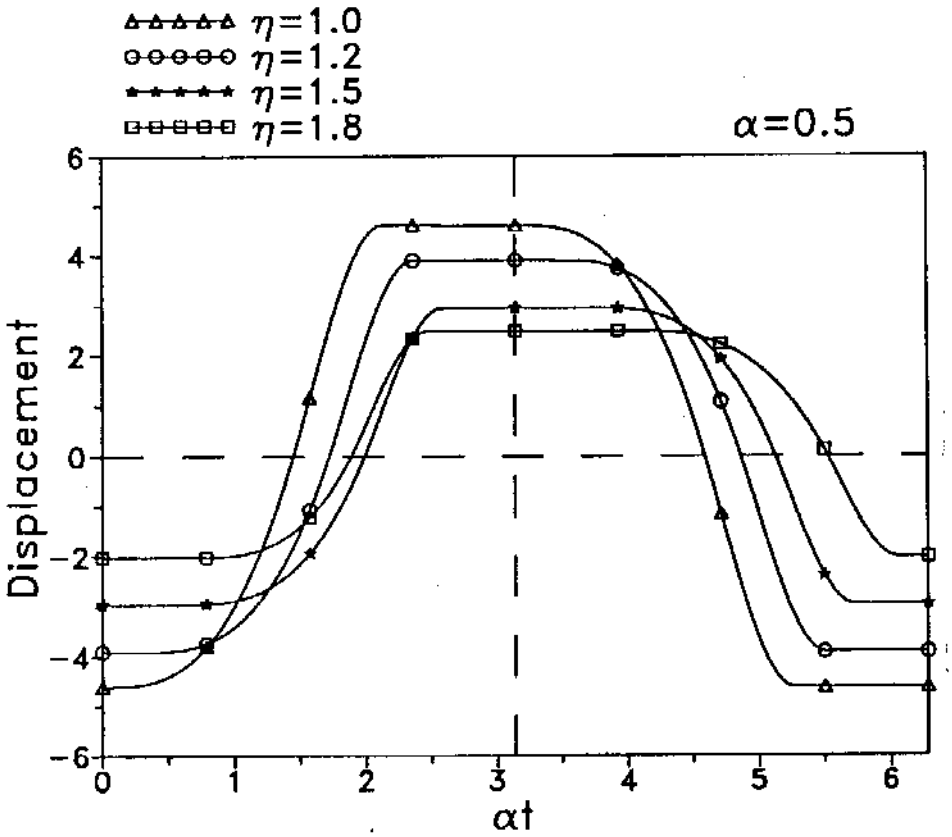

Fig.5: (b). displacement history

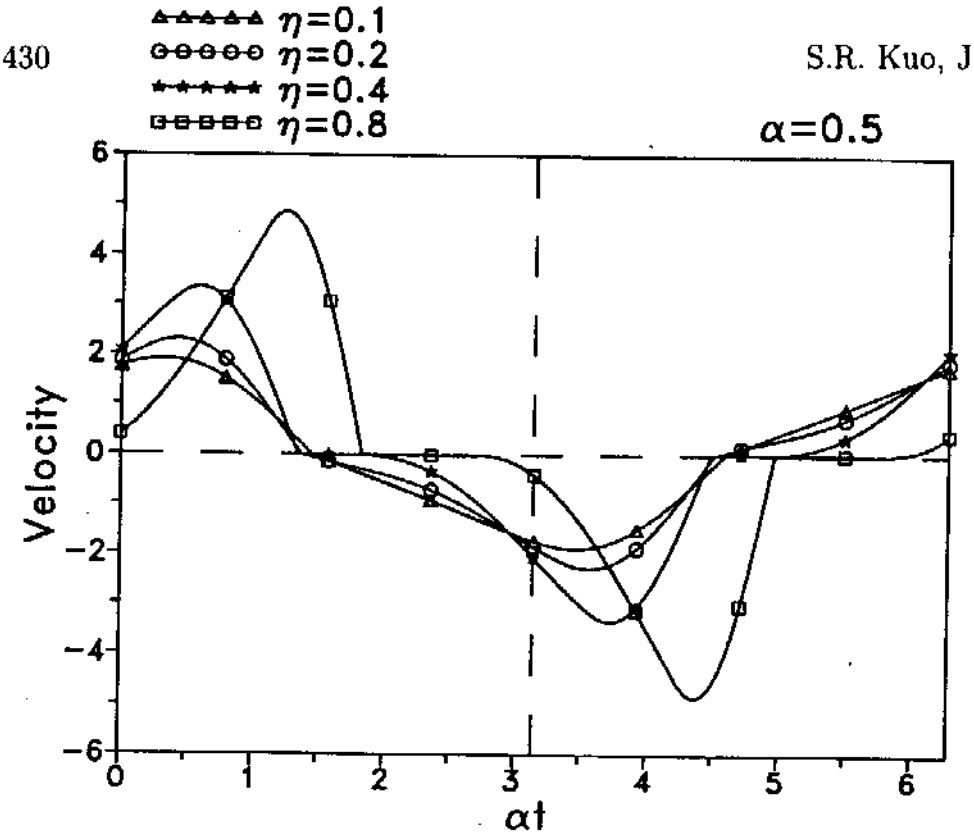

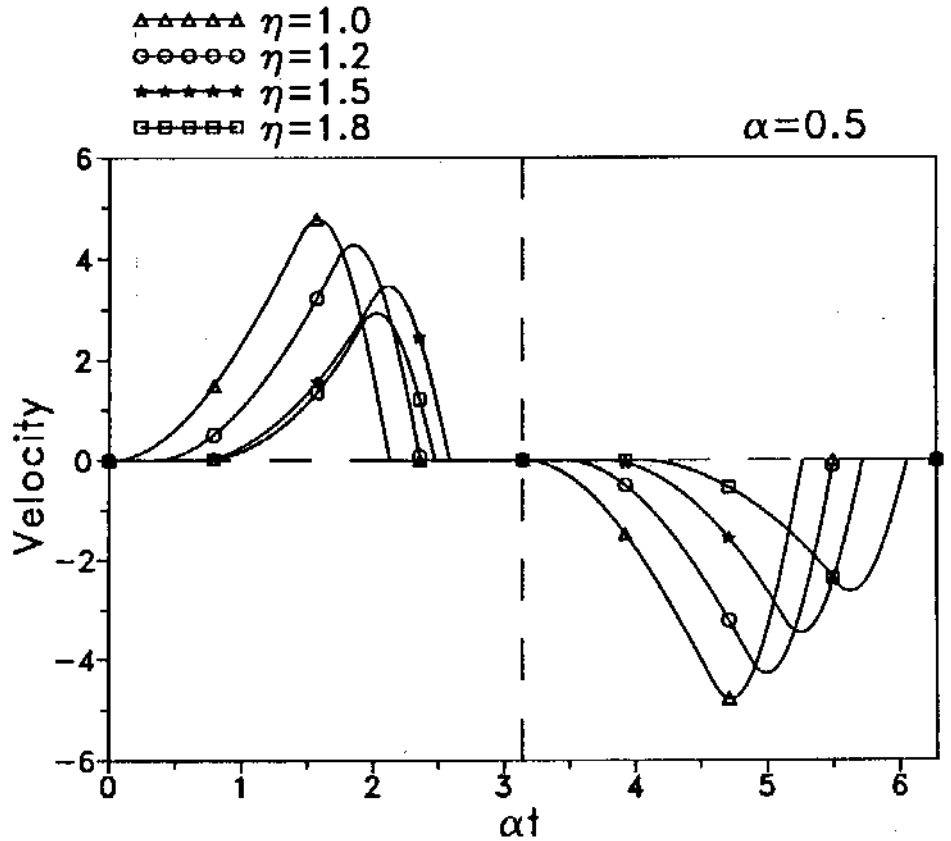

Fig.5: (c). velocity history for (1). $\eta = 0.1$, (2). $\eta = 0.2$, (3). $\eta = 0.4$, (4). $\eta = 0.8$. (5). $\eta = 1.0$, (6). $\eta = 1.2$, (7). $\eta = 1.5$, (8). $\eta = 1.8$.

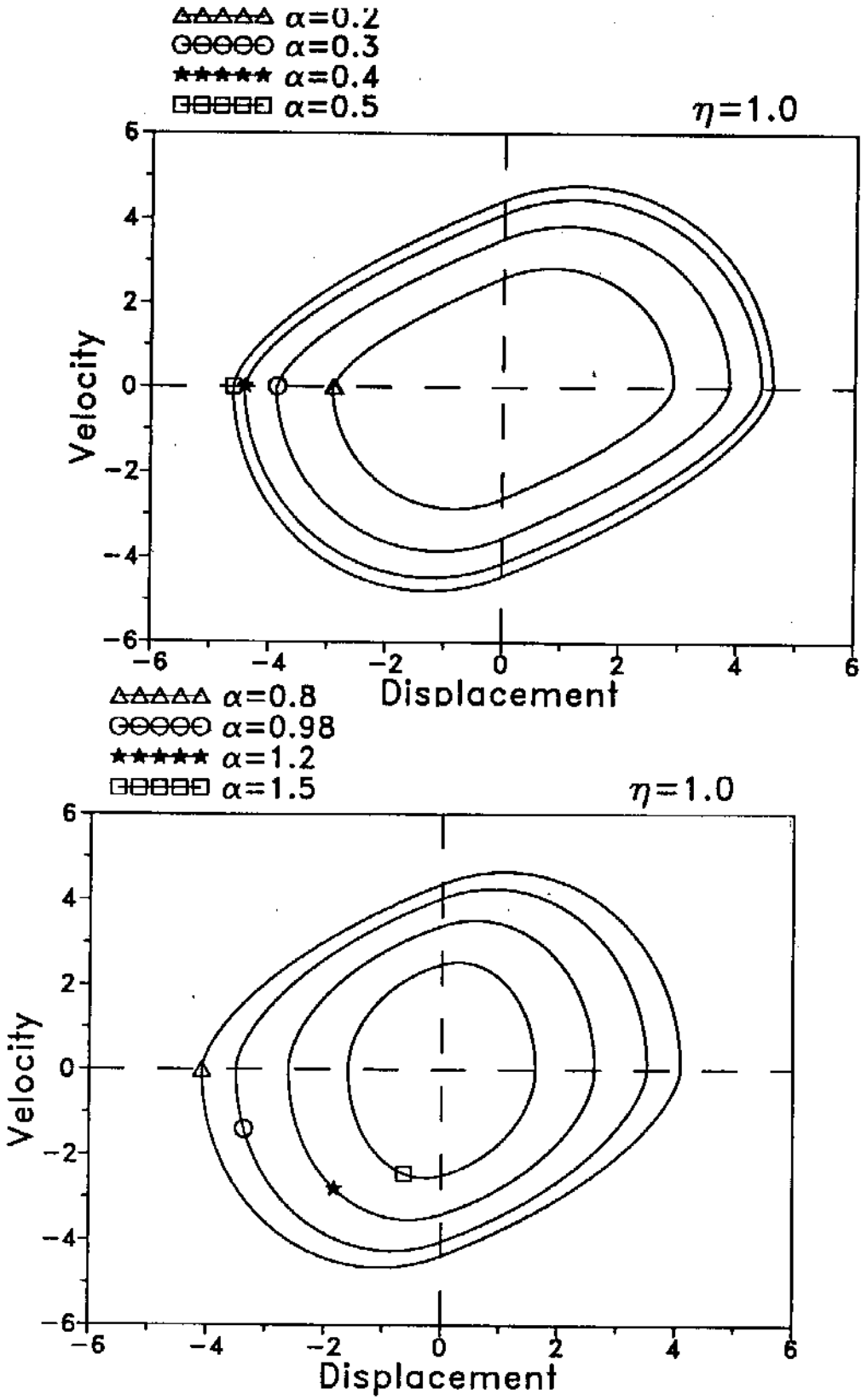

Fig.6: The phase lag between the input and output ($\eta = 1.0, \omega_0 = 1$).
(a). steady state trajectory in the phase plane

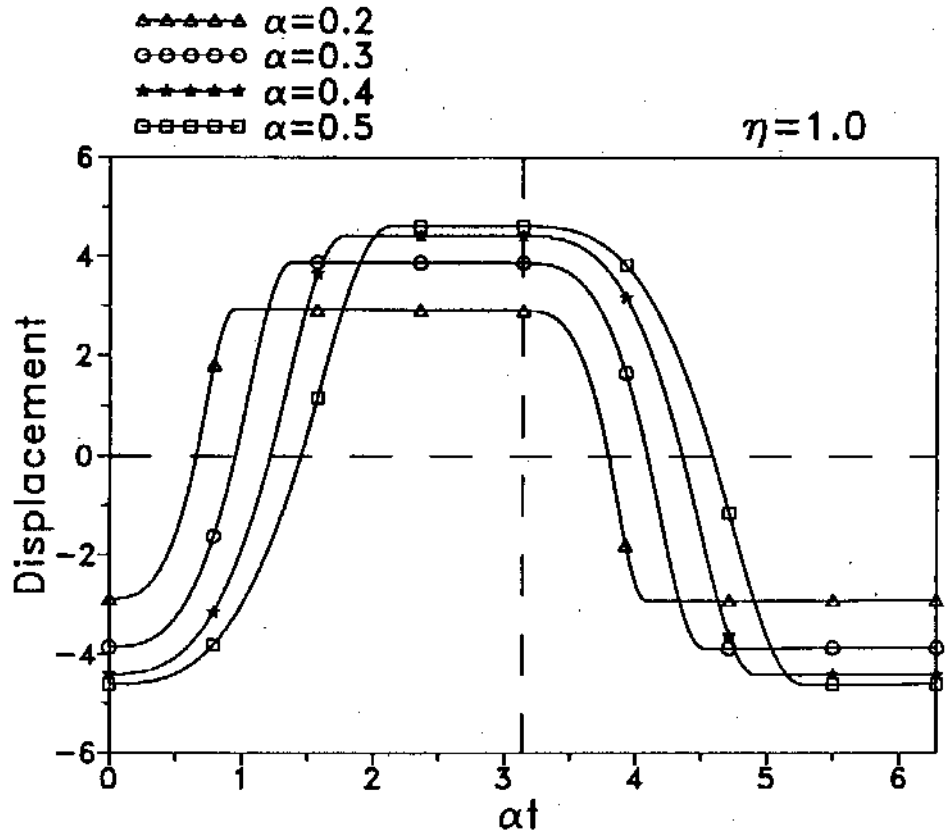

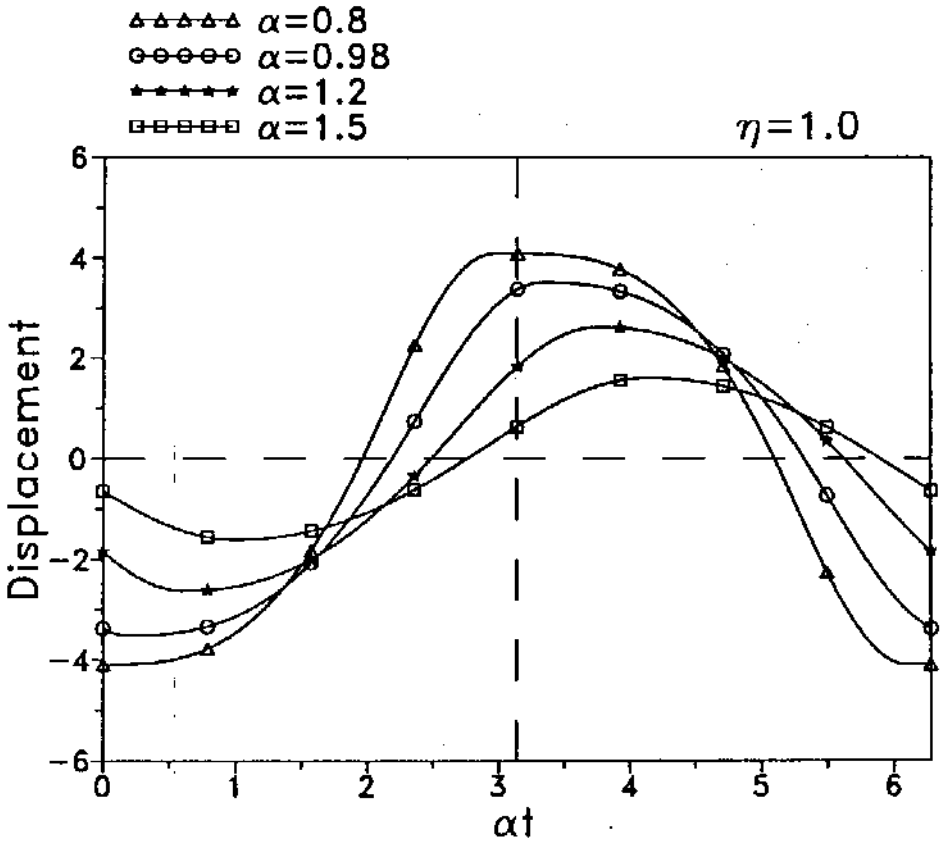

Fig.6: (b). displacement history

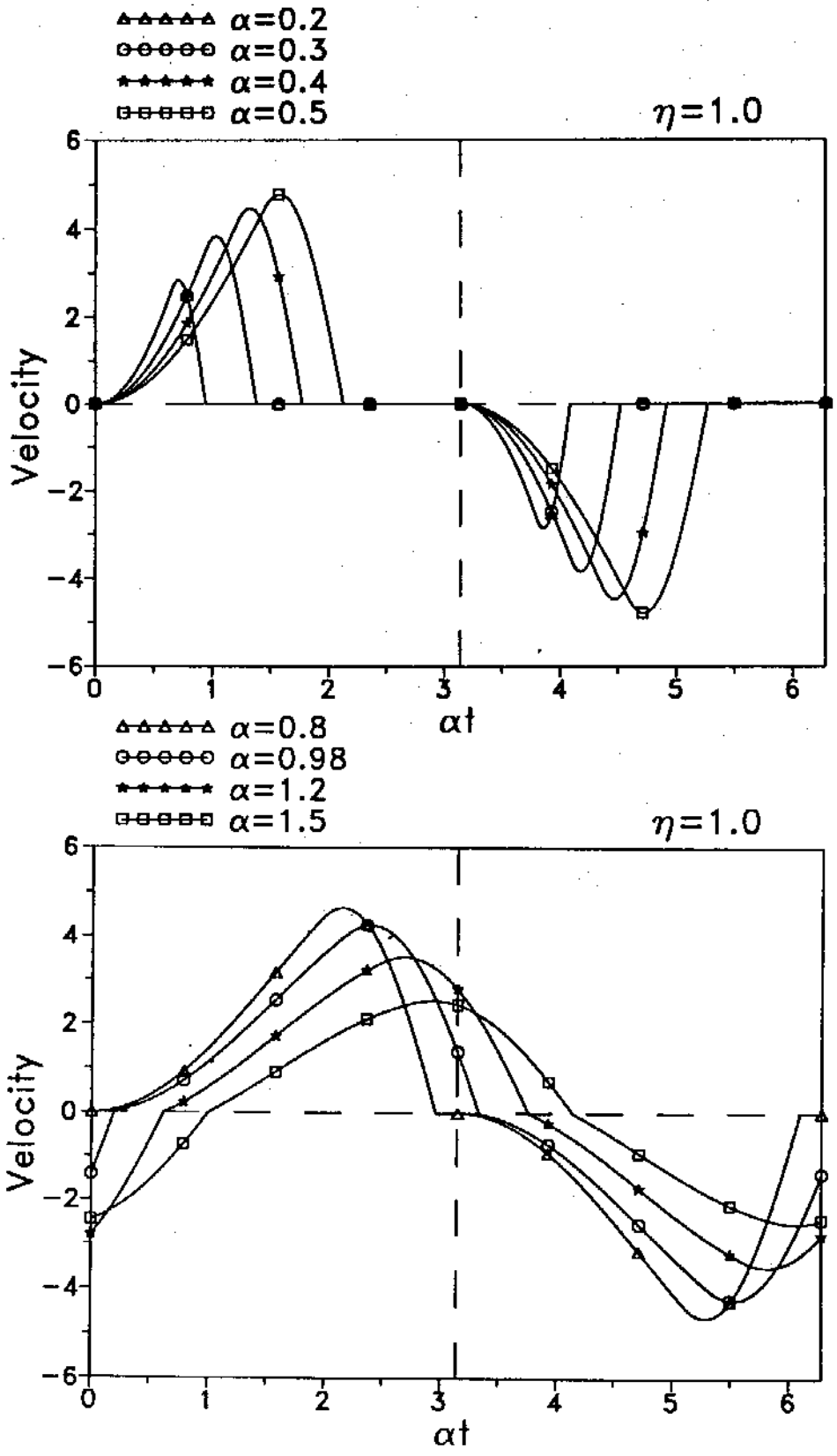

Fig.6: (c). velocity history for (1). $\alpha = 0.2$, (2). $\alpha = 0.3$, (3). $\alpha = 0.4$, (4). $\alpha = 0.5$, (5). $\alpha = 0.8$, (6). $\alpha = 0.98$, (7). $\alpha = 1.2$, (8). $\alpha = 1.5$

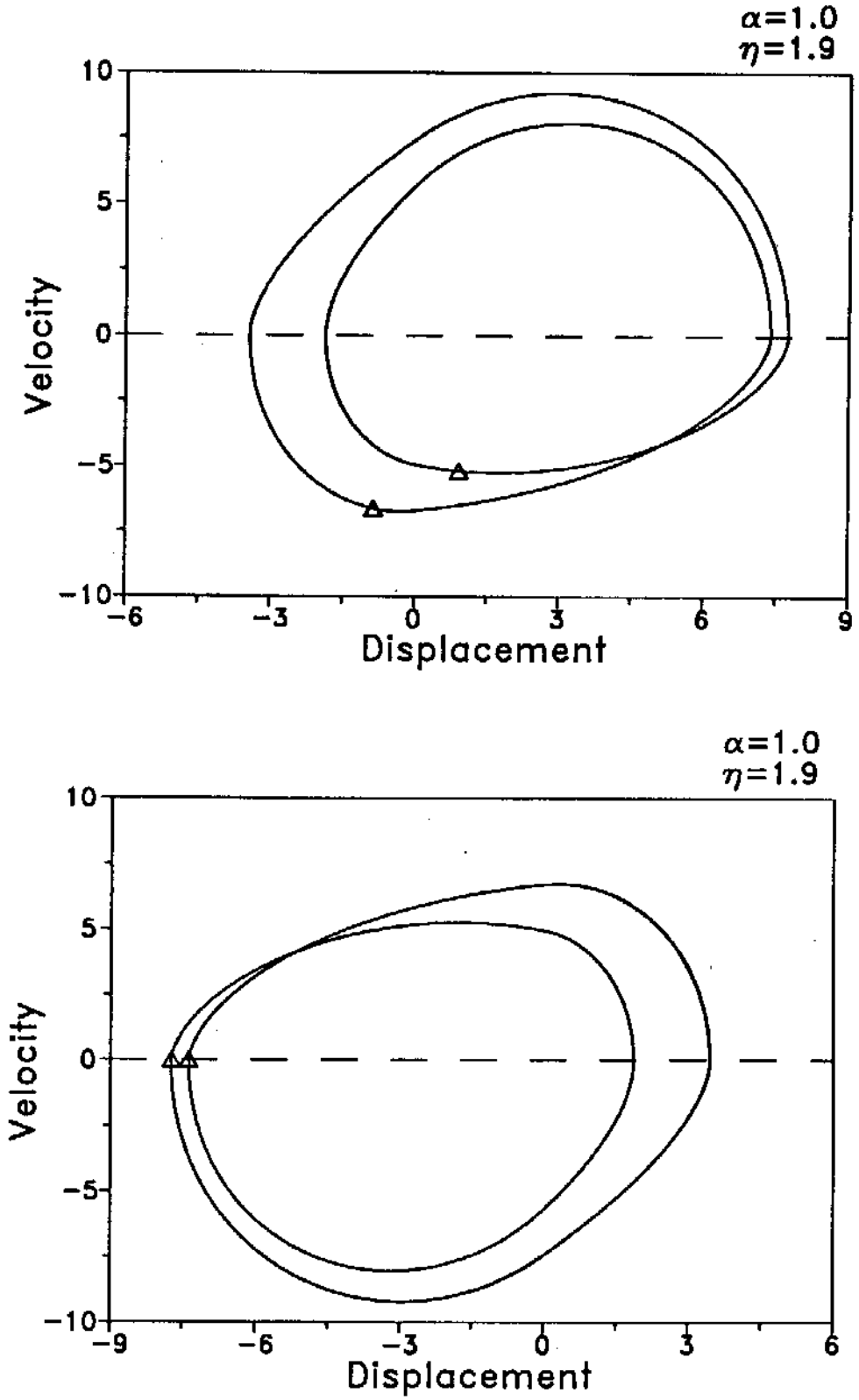

Fig.7: (a). The trajectory for subharmonic response ($\alpha = 1.0, \eta = 1.9$)

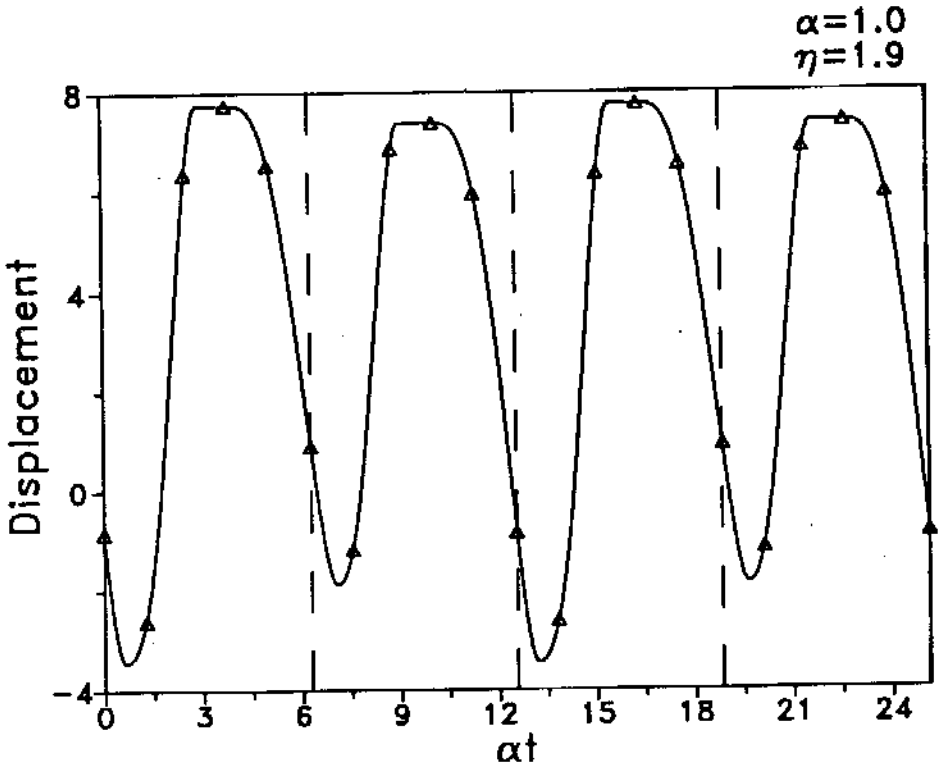

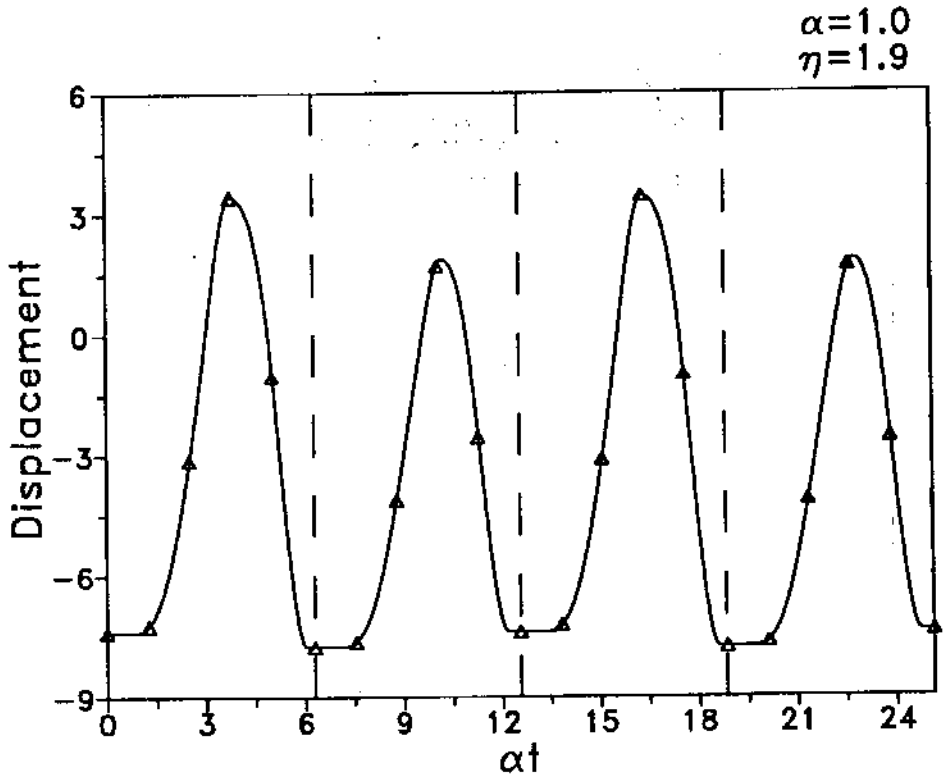

Fig.7: (b). The displacement history for subharmonic response

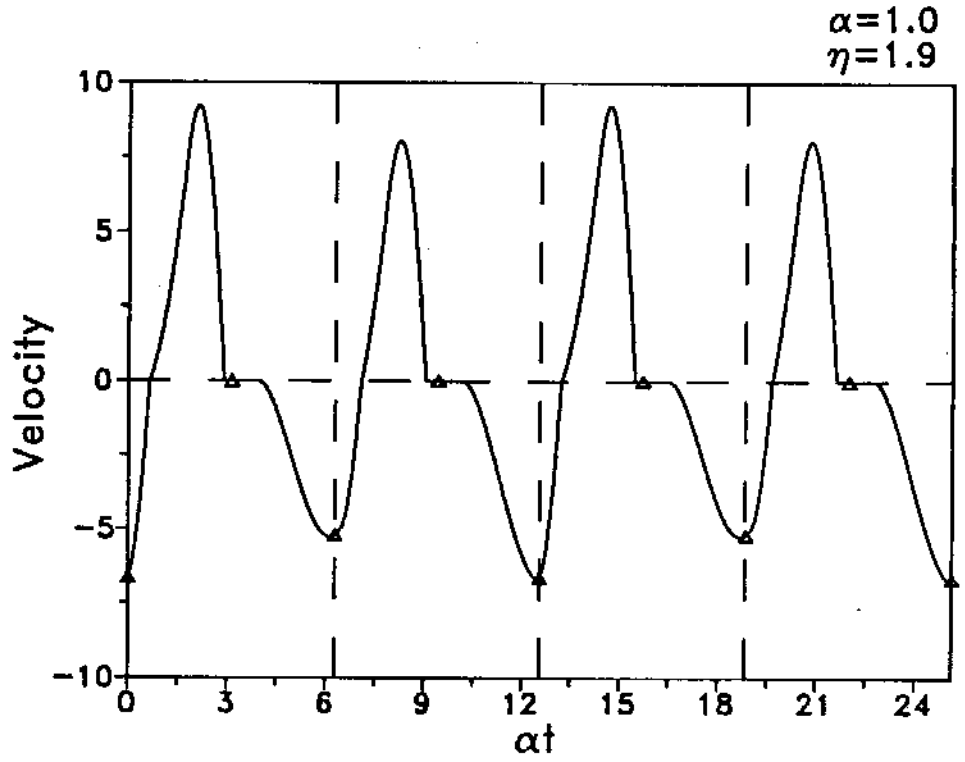

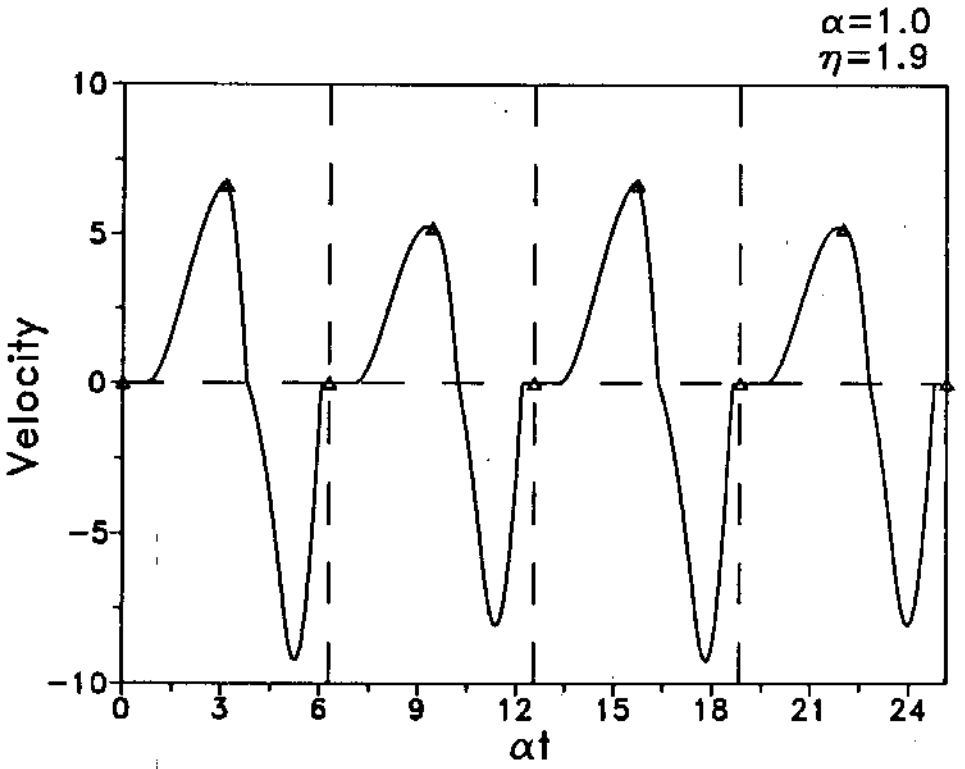

Fig.7: (c). The velocity history for subharmonic response

Table Captions:

Tab.1 Relation between the dissipation energy and loss factor.
Tab.2 Relation between the dissipation energy and exciting frequency.

Table 1: Dissipation energy of different loss factors with $p(t) = sin\pi t$ for the conventional and new hysteretic damping models.

Max. response ($\bar{X}_{max}$)	0.0351	0.0388	0.0487	0.0370
Max. response (X_{max})	0.0344	0.0326	0.0298	0.0231
Strain energy($V = \frac{1}{2}k\bar{X}^2_{max}$)	0.0243	0.0297	0.0468	0.0270
Strain energy($\bar{V} = \frac{1}{2}kX^2_{max}$)	0.022	0.021	0.0175	0.0105
Area of ellipse, dissipation energy ($\bar{W}$)	0.0153	0.0373	0.1177	0.1358
Area of ellipse, dissipation energy (W)	0.0138	0.0264	0.044	0.053
Loss factor ($\bar{\eta} = \frac{\bar{W}}{2\pi V}$)	0.1	0.2	0.4	0.8
Loss factor ($\eta = \frac{W}{4V}$)	0.05π	0.1π	0.2π	0.4π

Here, $\bar{\eta}$ and η are the loss factors defined for the nonlinear and linear hysteretic damping models, respectively. The parameters are shown below:

$\eta = \frac{\pi}{2}\bar{\eta}$, $m = 1kg, k = 4\pi^2 N/m^2, \omega_0 = 2\pi, \alpha = \pi$.

Table 2: Dissipation energy for the SDOF hysteretic system subjected to four different excitation frequencies, $\alpha = 0.5\pi$, $\alpha = \pi$, $\alpha = 1.5\pi$, $\alpha = 2\pi$, for $\bar{\eta} = 0.8$ and $p(t) = Asin\alpha t$.

	$\alpha = 0.5\pi$	$\alpha = \pi$	$\alpha = 1.5\pi$	$\alpha = 2\pi$
Amplitude ($\bar{A}$)	28.58	26.99	31.71	38.61
Amplitude (A)	48.65	43.29	36.00	31.58
Max. response ($\bar{X}_{max}$)	1	1	1	1
Max. response (X_{max})	1	1	1	1
Strain energy($V = \frac{1}{2}kX^2_{max}$)	19.78	19.78	19.78	19.78
Strain energy($\bar{V} = \frac{1}{2}kX^2_{max}$)	19.74	19.74	19.74	19.74
Area of ellipse, dissipation energy ($\bar{W}$)	99.22	99.22	99.22	99.22
Area of ellipse, dissipation energy (W)	99.22	99.22	99.22	99.22
Loss factor ($\bar{\eta} = \frac{\bar{W}}{2\pi V}$)	0.8	0.8	0.8	0.8
Loss factor ($\eta = \frac{W}{4V}$)	0.4π	0.4π	0.4π	0.4π

References

[1] L.Y. Chen, J.T. Chen, C.H. Chen & H.-K. Hong, Free vibration of SDOF system, *Mech. Res. Comm.*, **21** (1994), 599-604.

[2] S.H. Crandall, A new hysteretic damping model? *Mech. Res. Comm.*, **22** (1995), 201-202.

[3] N. Makris and M.C. Constantinou, Analysis of motion resisted by friction, Part I: Constant Coulomb and linear/Coulomb friction, *Mech. Struc. & Mach.*, **69** (1991), 477-500.

[4] K.K. Beucke and J.M. Kelly, Equivalent linearization for practical hysteretic systems, *Int. J. Nonlinear Mechanics*, **32** (1985), 211-238.

[5] J.T. Chen and D.W. You, Integral-differential equation approach for the free vibration of a SDOF system with hysteretic damping, *Advances in Engineering Softwares*, **30** (1999), 43-48.

[6] J.T. Chen and D.W. You, Hysteretic damping revisited, *Advances in Engineering Software*, **28** (1997), 165-171.

[7] J.A. Inaudi and J.M. Kelly, Linear hysteretic damping and the Hilbert transform, *J. of Engineering Mechanics, ASCE*, **121** (1995), 662-632.

[8] T.K. Caughey and A. Vijayaraghavan, Free and forced oscillations of a dynamic system with "linear hysteretic damping" (nonlinear theory), *Int. J. Nonlinear Mechanics*, **5** (1970), 533-555.

[9] R.W. Clough and J. Penzien, *Dynamics of Structures*, McGraw-Hill, New York (1975).

[10] A.D. Nashif, D.I.G. Jones and J.P. Henderson, *Vibration Damping*, John Wiley & Sons, New York (1984).

[11] N.O. Myklestad, The concept of complex damping, *J. Appl. Mech.*, **19** (1952), 284-286.

[12] R.E.D. Bishop, The treatment of damping force in vibration theory, *J. Royal Aeronautical Society*, **59** (1955), 738-742.

[13] P. Lancaster, Free vibration and hysteretic damping, *J. Royal Aeronautical Society*, **64** (1960), 229-229.

[14] R.E.D. Bishop and W.G. Price, A note on hysteretic damping of transient motions, In:*Random Vibration – Status and Recent Development*, Ed. by I. Elishakoff and R.H. Lyon, Elsevier, Amsterdam (1986).

[15] L. Meirovitch, *Elements of Vibration Analysis*, McGraw-Hill, Singapore (1986).